

Performance Investigation of Carbon Nanotube Based Temperature Compensated Piezoresistive Pressure Sensor

REKHA DEVI (✉ rekha.e8517@cumail.in)

Chandigarh University

Sandeep Singh Gill

NITTTR Chandigarh

Research Article

Keywords: MEMS, Piezoresistive pressure sensor, silicon, sensitivity, Linearity, Diaphragm, CNT

Posted Date: February 17th, 2021

DOI: <https://doi.org/10.21203/rs.3.rs-203435/v1>

License:  This work is licensed under a Creative Commons Attribution 4.0 International License.

[Read Full License](#)

Performance investigation of Carbon nanotube based temperature compensated piezoresistive pressure Sensor

Rekha Devi^{1*} and Sandeep Singh Gill²

¹ IKG Punjab Technical University, Jalandhar India

¹ Chandigarh University, Mohali, India

² National Institute for Technical Teachers Training & Research Chandigarh, India

*rekha.e8517@cumail.in

Abstract: In silicon-based piezoresistive pressure sensor, the accuracy of the sensor is affected mainly by thermal drift and the sensitivity of the sensor varies with the rise in temperature. Here, the temperature effects on the desired representation of the sensor are analysed. Use of smart material Carbon nanotubes (CNT) and a few effective temperature compensation techniques are presented in this study to reduce the temperature effect on the accuracy of the sensor. Resistive compensation employed extra piezoresistors with Negative Temperature Coefficient of Resistivity (TCR) for temperature compensation. The attainment of the desired compensation techniques is highly compatible with the MEMS device fabrication. The compensated pressure sensor is supremacy for pressure measurement with temperature variations. Though various techniques have been suggested and put into actuality with successful attainment, the techniques featuring easy implementation and perfect compatibility with existing schemes are still blooming demanded to design a piezoresistive pressure sensor with perfect comprehensive performance.

In this paper, CNT piezoresistive material has been employed as sensing elements for pressure sensor and compared with silicon in terms of output voltage and sensor performance degradation at higher temperature. Pressure sensors using CNT and silicon piezo resistive sensing materials were simulated on silicon (100) diaphragm by ANSYS. Based on simulation results, silicon and CNT both pressure sensor also shows better results at near room temperature. With the increasing temperature it is observed that silicon pressure output underestimated by 23%.

Keywords MEMS, Piezoresistive pressure sensor, silicon, sensitivity, Linearity, Diaphragm, CNT.

1.Introduction: Micro Electro Mechanical Systems (MEMS) based pressure sensors, find various biomedical applications such as measuring the outlet and inlet pressures of blood, monitoring intrauterine pressure (IUP), intracranial pressure ICP, and intra-ocular pressure IOP [1-5]. Piezoresistive property in semiconductor materials is mainly applied in pressure sensors as well in others like cantilever force sensors, inertial sensors, and accelerometers. This is the phenomenon by which the change in electrical resistance of the material in response to applied mechanical stress is declared as piezoresistivity [6]. The piezoresistive properties of germanium and silicon were found by smith in the 1954 phenomenon [7]. Four piezoresistors are assembled through electric connections and put in Wheatstone bridge arrangement to transducer the change in resistance into output voltage. Due to the high sensitivity of Polysilicon material to change in strain then metal was used for MEMS sensor, however, its response is highly temperatures dependent [8]. The response of the piezoresistor is determined mainly by the temperature coefficient and the doping concentration of the piezo-resistive coefficient.

Some other important aspects are also affected by temperature [9]. Slight variation in temperature may lead to major drift in acquired signal. For the piezoresistive sensor many temperature compensation methods have been implemented [31]. CNTs materials are used to design MEMS sensors due to their outstanding mechanical and electrical properties. CNTs are the encouraging Nano-structured material to be suggested in the field of micro-sensing technology. CNTs have a tensile strength of 60 GPa and gauge factor to be about ~ 1000 [16]. CNTs material has a great property of elasticity almost 1 TPa [10]. Downscaling of diaphragm-based Piezoresistive pressure sensors becomes possible by replacing Si with SWCNTs and that the miniaturized sensors defeated Si concerning power consumption, sensitivity, and size [11]. CNTs have some advantages instead of other materials that the sensor based on CNT is not fabricated at high temperature and the response of the sensors are independent of temperature. The piezoresistive sensors undergo the disadvantage that the sensor output is highly affected with variation in temperature, which leads to sensitivity drift and thermal zero shift. The fabrication and packaging of sensors are often under high-temperature conditions. The temperature effect on the piezoresistive coefficient and resistance, due to the fabrication process the thermal residual stress, and the chip packaging, the residual stress are the main contributing factors in these [12]. Analyzed the response of CNT based pressure sensors for high temperature and pressure [13]. Silicon piezoresistive pressure sensors recently make use of MEMS Technology for the fabrication. Temperature affects the sensitivity of silicon piezoresistive sensors [14]. For the Design of a good quality pressure sensor, the temperature effects of the piezoresistive pressure sensor must well be known.

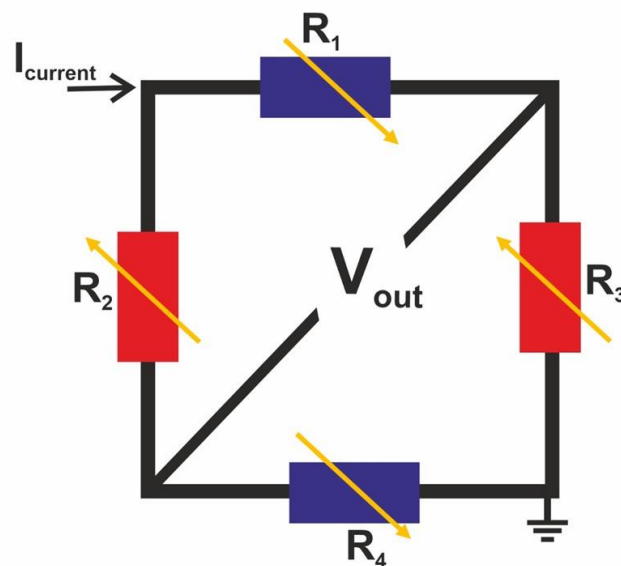


Figure 1. Equivalent Circuit of the piezoresistive pressure sensor

2. Temperature Effects of the Piezoresistive MEMS Pressure Sensor

With the applied pressure, the sensor's diaphragm will deform which induce bending of stresses in the piezoresistors and translate into a fluctuation in the resistance because of the piezoresistive effect[15]. Piezoresistive MEMS pressure sensors suffered from a major problem of implicit decline sensitivity to temperature. Piezoresistors in the form of wheatstone bridge configuration were placed to convert applied pressure into electrical signal as shown in figure 1.[32-33]. In these sensors the resistance of Transversal piezoresistor and longitudinal piezoresistor on silicon diaphragm due to thermal expansion the diaphragm deflection taking into account. Induced stress σ and change resistance are given by piezoresistive coefficient π can be defined as.

$$R(T) = R_{Tr} + \Delta R(T) + \Delta R(\sigma(T), \pi(T)) \quad (1)$$

Where first, second, and the third term of this equation (1) can be written as

$$R_{Tr} = \rho_r \frac{L}{A} \quad (1a.)$$

$$\Delta R(T) = R_{Tr} \alpha_r \Delta T \quad (1b.)$$

$$\Delta R(\sigma(T), \pi(T)) = R_{Tr} (\sigma_T(T) \pi_T(T) + \sigma_L(T) \pi_L(T)) \quad (1c.)$$

$$\Delta T = T_o - T_r \quad (1d.)$$

ρ_r is the isotropic resistivity at reference temperature T_r for the unstressed crystal, R_{Tr} is the resistance of the piezoresistors diffused on the substrate, T and L indicate Transverse and a longitudinal direction of induced mechanical stress to the current I respectively, ΔT is the difference in temperature between the operating temperature and reference temperature T_f (the reference temperature is usually 0°C).

2. Temperature impact on the Piezoresistor and Piezoresistive coefficient

In the absence of the applied pressure to the diaphragm, the resistance of the four piezoresistors is exactly matched and the output voltage (V_{out}) of the sensor must be zero. However, the temperature rise can vary the resistance values of all the piezoresistors; therefore, the offset voltage will change. The resistance of the piezoresistors influence by the temperature is described below [21].

$$R_n(T, \sigma) = R_{n,0} (1 + \alpha_n \Delta T + \beta_n \Delta T^2) + R_{n,0} \pi_{44} (1 + \delta_n T) \Delta \sigma_n \quad (2)$$

Where $R_{n,0}$ is the initial resistance of n number of the piezoresistive element (1, 2, 3, and 4), α_n and β_n are the temperature coefficients of resistivity (TCR), $\delta_n T$ is referred to as the thermally-induced change of piezoresistive coefficient, the temperature coefficient of sensitivity (TCS) is mainly determined by this, σ_n is the change in transverse and longitudinal stress. If the circuit is intersecting into two different parts, the left-hand part with resistor R_{L1} and R_{T1} . The change in output Voltage of this part at temperature T is calculated by

$$\frac{V_{oL1T1}(T)}{V_{in}} = \frac{R_{T1}(T)}{R_{L1}(T) + R_{T1}(T)} \quad (3)$$

The ratio of change in output voltage to input voltage in the left part at temperature T is given as

$$\frac{\Delta V_{O,T_1L_1}(T)}{V_{in}} = \frac{R_{0,T_1}}{R_{0,T_1}+R_{0,L_1}} - \frac{R_{T_1}(T)}{R_{T_1}(T)+R_{T_1}(T)} = \frac{R_{0,T_1}R_{0,L_1}}{(R_{0,T_1}-R_{0,L_1})^2} [(\alpha_1 - \alpha_2)\Delta T - (\beta_1 - \beta_2)\Delta T^2] \quad (4)$$

In the zero-offset voltage, the resulting temperature variation can be written as

$$\frac{V_{offset}(T)}{V_{in}} = \frac{R_{0,T_1}R_{0,L_1}}{(R_{0,T_1}+R_{0,L_1})^2} [(\alpha_1 - \alpha_2)\Delta T + (\beta_1 - \beta_2)\Delta T^2] - \frac{R_{0,T_2}R_{0,L_2}}{(R_{0,T_3}+R_{0,L_4})^2} [(\alpha_3 - \alpha_4)\Delta T + (\beta_3 - \beta_4)\Delta T^2] \quad (5)$$

When no pressure is applied, the overall reactance of all the four piezoresistor is equal and is expressed by R_0 .

$$\frac{V_{offset}(T)}{V_{in}} = \frac{1}{4} \sum_{n=1}^4 -1^{n+1} [(\alpha_n)\Delta T + (\beta_n)\Delta T^2] \quad (6)$$

The piezoresistive coefficient of silicon π_{44} is a function of doping concentration and temperature represented as $f(N, T)$, where T is temperature and N is doping concentration [22]

$$\pi_{44}(N_D, T) = \pi_{44}(N_{0D}, 300 K)P(N_D, T) \quad (7)$$

Where $\pi_{44}(N_{0D}, 300 K)$ is the piezoresistive coefficient expressed at room temperature. $P(N_D, T)$ is the piezoresistive factor depending on doping concentration as well as the temperature and TCS and TCR coefficient can be defined in equation [23-25].

$$P(N_D, T) = \frac{300}{T} \frac{1}{\left(1 + \exp\left(-\frac{E_F}{K_B T}\right)\right) \ln\left(1 + \exp\left(\frac{E_F}{K_B T}\right)\right)} \quad (8)$$

$$TCS = \frac{d\pi(N_D, T)}{\pi dT} 10^6 \quad (9)$$

$$TCR = \frac{dR}{dT} 10^6 = \frac{dV}{dT} 10^6 \quad (10)$$

Where E_F and K_B are the Fermi level energy of silicon and the Boltzmann constant respectively. The output voltage of the sensor in terms of operating temperature T and Stress (σ) can be expressed as following

$$\frac{V_{out}(T)}{V_{in}} = \frac{1}{2} \pi_{44}(N_{0D}, 300 K)P(N_D, T)(\sigma_L - \sigma_T) + V_{offset}(T) \quad (11)$$

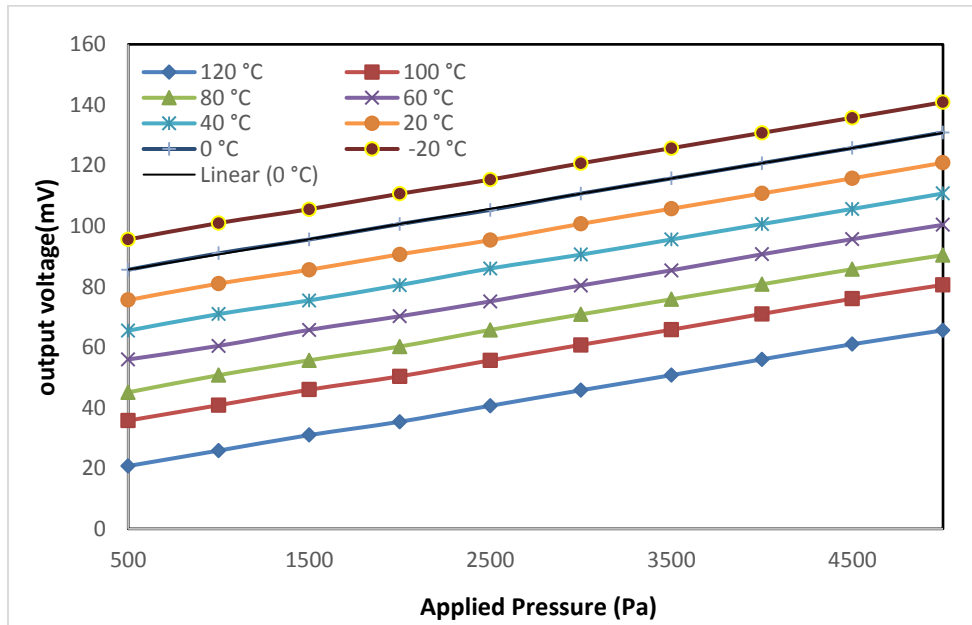
The first term in (11) represents the temperature effect on piezoresistive coefficients and the second term represents offset voltage induced by TCR.

3. The sensitivity of the pressure sensor Influence by the Doping Concentration

The most important performance parameter of the sensor is the sensitivity and the doping concentration is a factor of piezoresistive pressure sensors, which greatly affects the sensitivity. The dependency of the sensitivity on doping concentration is calculated using the following equation [26].where a is length and h is the thickness of the diaphragms.

$$S(T, N) = \frac{\pi_{44}(N, T)}{2} \left(\frac{a}{h}\right)^2 (\sigma_L - \sigma_T) \quad (12)$$

The response of the sensor is examined within the temperature range from -20°C to 120°C, which is a practicable range for most biomedical applications. Figure 2. Shows the Relationship between the output voltage and the applied pressure under various temperatures. The results indicate that the output voltage shrinks at a higher temperature range. Figure 3. Illustrates that with the increase in temperature, there will drop in sensitivity due to a decrease in temperature coefficient. Compared with the sensitivity at room temperature (20 °C), this drop of sensitivity is around 26% at 120°C. The non-linearity of the sensor is plotted in figure 4. The antithesis to the Sensitivity decay, the linearity parameter improves at higher temperatures.



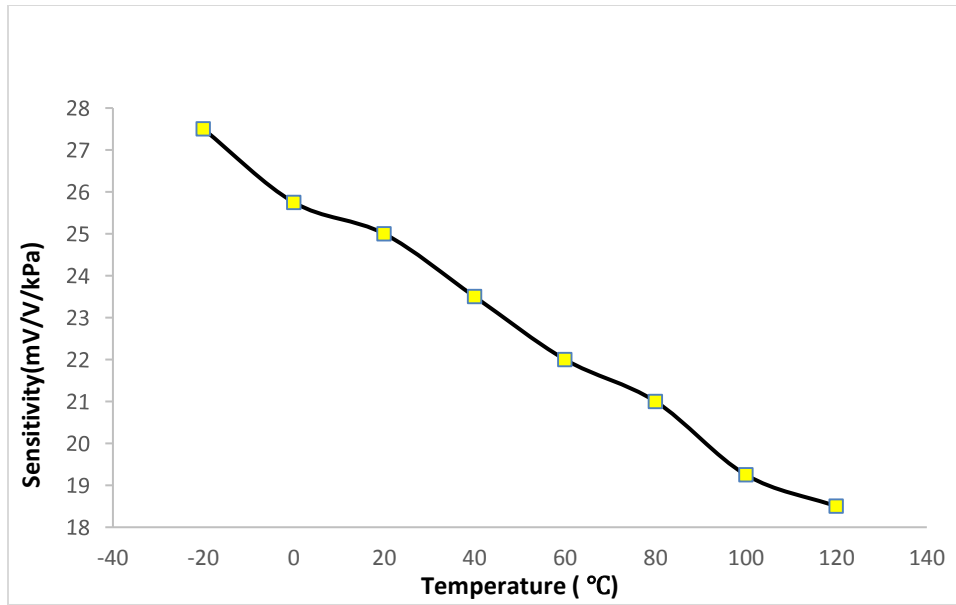


Figure 3. The relationship plot between the sensitivity of the pressure sensor and temperature variations.

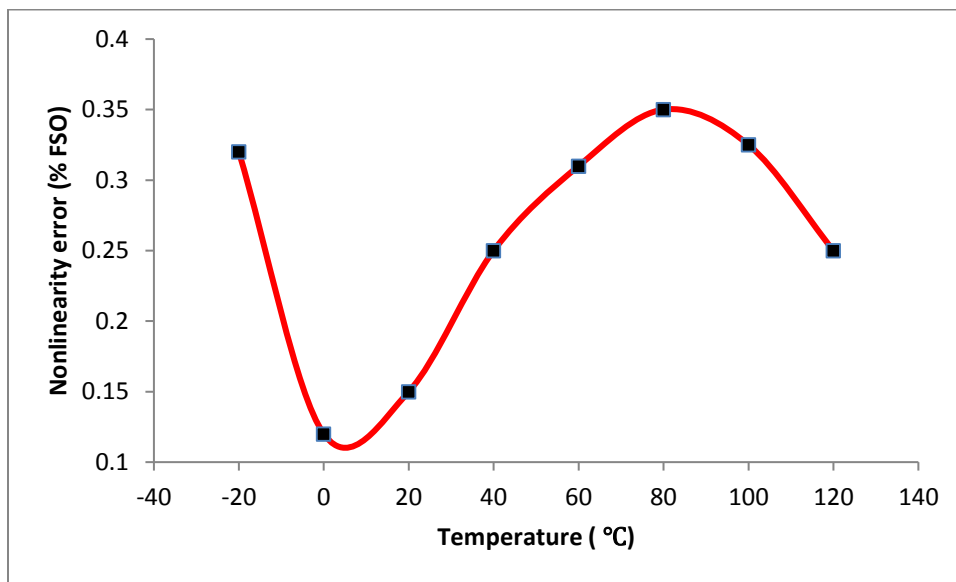


Figure 4. Nonlinearity error measurement of the pressure sensor and temperature variations.

4. CNT piezoresistive sensing material based

The pressure sensitivity due to temperature expansion were taken into the considered . The simulation results of silicon and CNT material for pressure range 500 to 5000 pascal and temperature range 20°C to 60°C using Ansys plotted in figure 5 . silicon material shows better results at lower temperature (near room temperature) but its performance starts reducing with the increase in temperature . CNT shows good temperature compatibility due to its high temperature conductivity in varied temperature range. Use of CNT material as piezoresistive sensing elements

in preeure sensor shows good result as compared to silicon material at all temperature ranges .With CNT material , the overall sensitivity of the sensor is improved.

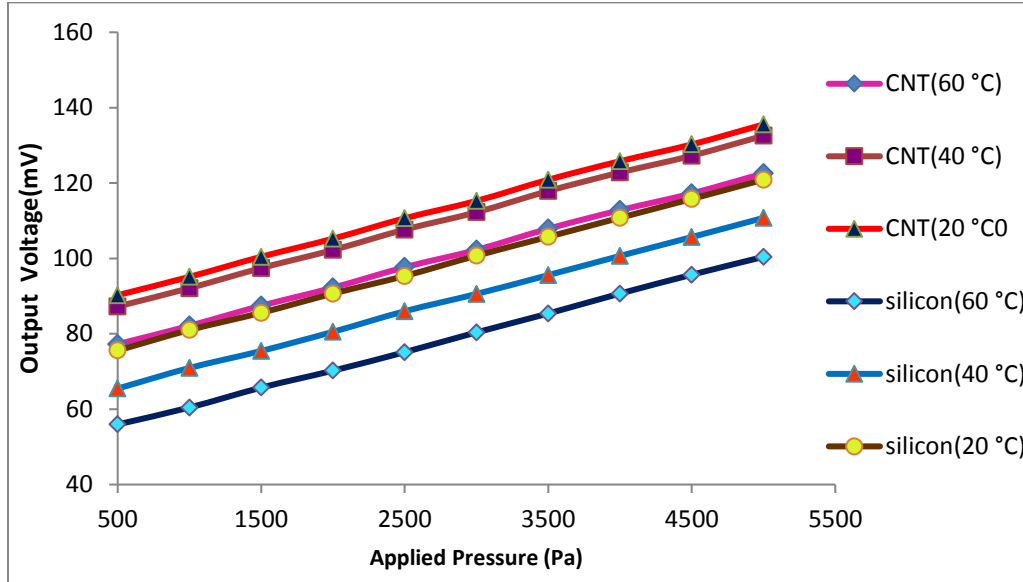


Figure 5 . Comparative analysis of silicon and CNT as piezoresistive sensing elements at different temperature range.

5.Design of compensation circuit:

Piezoresistive pressure sensor for higher temperature following the Wheatstone bridge configuration continues to drop in the sensor's sensitivity is assured, because of increase piezoresistance and decrease in piezoresistive coffiecnt. Thus the testing accuracy is adversely affected by these phenomenons. Software compensation, Hardware compensation, and hybrid approaches are three commonly used compensation techniques [30]. software compensation has more accuracy but required high testing cost and complex circuitry. whereas in hardware compensation, because of circuit simplicity, lower cost, more reliability, more economical, more efficiency, higher accuracy, batch fabrication, a wide range of applications, has been used. Hardware compensation needed additional diode, diode, thermisters, operational amplifiers, and resistive network with a low-temperature coefficient [27-28].

5.1.Resistive compensation network

Resistive network for low-temperature coefficient, temperature compensation technique used for sensor design based on hardware compensation as shown in the figure 6. A constant input voltage source (V_{in}) is applied as input to the bridge circuit and R_{TCS} , R_{TCO} , and R_Z registers are added as a compensator for compensating TCS, TCO, and zero-offset respectively [28]. At

least the resistance of one piezoresistor is temperature dependant. To expedite the compensation for zero-offset, the Wheatstone bridge circuit can be constructed into a half open-loop. Setting I_n as excitation input current and $V_{(z-off)}$ the zero-offset voltage, the value of R_Z can be calculated by the expression given below.

$$R_Z \approx \frac{4|V_{(z-off)}|}{I_{in}} \quad (13)$$

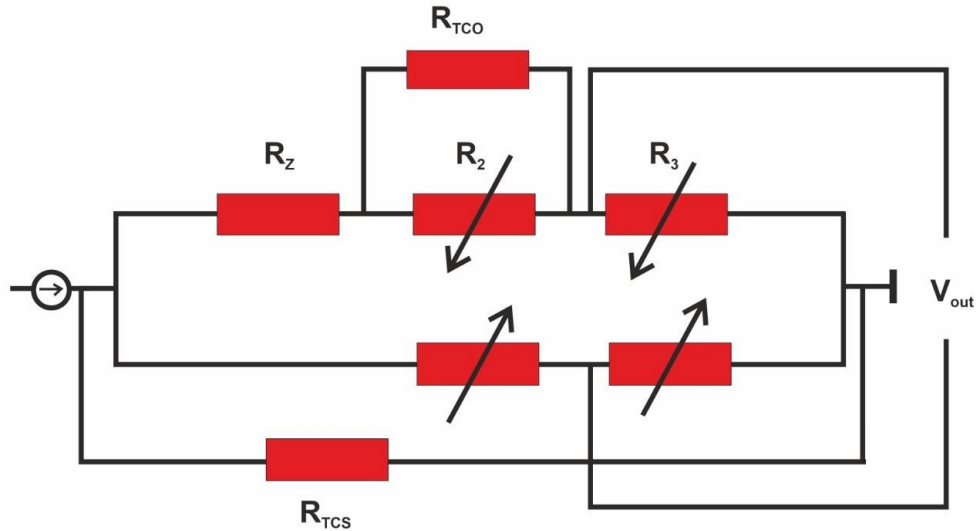


Figure 6 .Schematic diagram of the resistive compensation network.

If $V_{(z-off)} > 0$, R_Z should be placed with the arm R_2 in the bridge circuit. The resistance of the TCS and TCO compensation can be expressed as.

$$R_{TCS} \approx \left| \frac{TCS_0}{TCS_0 + TCR_b} \right| R_b \quad (14)$$

Where TCS_0 is TCS without compensation and TCR_b , R_b is the bridge TCS and resistance respectively.

$$R_{TCO} \approx \frac{I_{in}(R_{t_2}^2 - R_{t_1}^2)}{4|\Delta V_{(z-off)}|} \quad (15)$$

Where R_{t_2} and R_{t_1} are the average resistance at temperature t_2 and t_1 respectively, $\Delta V_{(z-off)}$ is the change in offset voltage at temperature t_2 and t_1 . To make the compensation reliable and effective, all three compensation registers should be used with a low resistive temperature coefficient.

5.2. Temperature Compensation using Double Bridge Circuit

The circuit diagram of double bridge temperature compensation techniques is shown in the figure 7. A bridge of piezo resistors is placed on the diaphragm and the output of this bridge is the function of temperature and pressure. The response of the compensation bridge circuit is temperature-dependent only. The size and the shape of the resistor used in the compensation bridge are identical to the piezoresistor used as sensing elements. Op-Amp (1) and Op-Amp (2) used as a differential amplifier to convert the dual output of bridge networks into a single output, Op-Amp (3) is used as a subtractor to produce the difference in the output of two bridges circuits. Analog to Digital converter (ADC) is used to digitized the output obtained from Op-Amp (3) for further processing to obtain a temperature compensated output(digital). Double bridge temperature compensation technique is simulated for a temperature range - 20°C to 120°C, shows encouraging results of zero-offset voltage for bridge compensation.

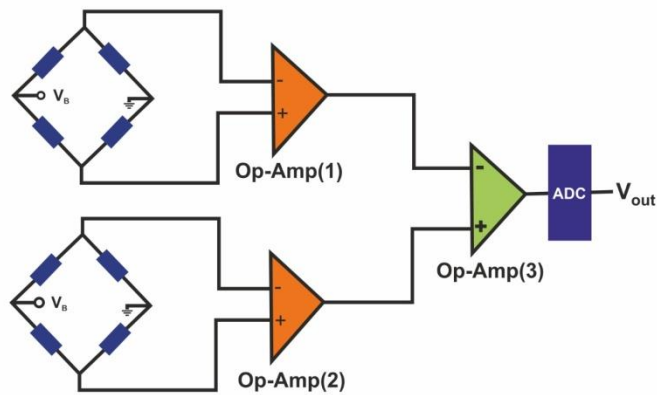


Figure 7 .Schematic diagram of the Double bridge compensation network.

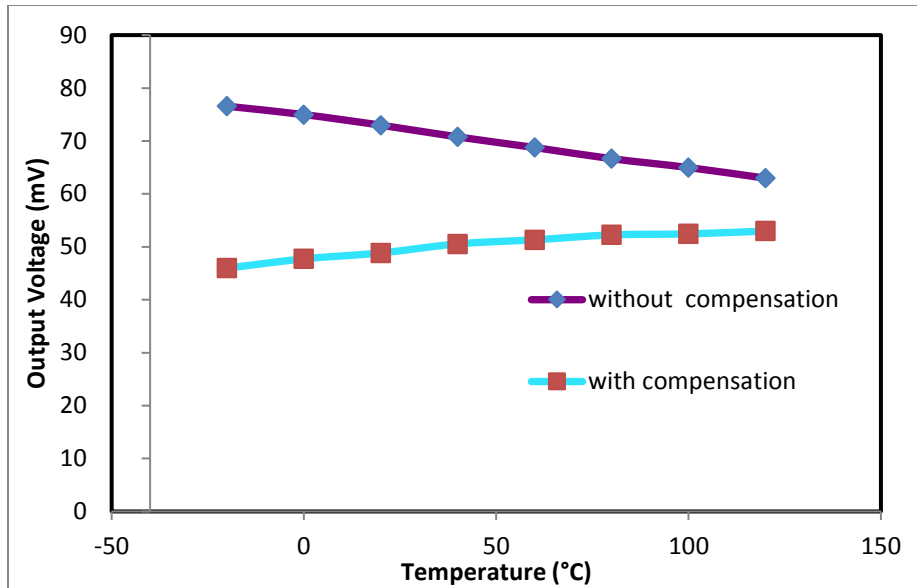


Figure 8 . Output voltage with compensated and without compensated pressure sensor vs. temperature.

Figure 8 shows the simulation results of output voltage for different temperature range with compensation circuits and without compensation circuit with same pressure , output voltage without compensation is decreasing with the increase in temperature which is responsible for the drop in sensitivity but with the compensation ,output voltage remains constant with the increase in temperature .

6.Conclusion: In this Research , the temperature effect on the output voltage of a Piezoresistive pressure sensor has been examined through analysis of the temperature influence on the resistances of registers . It can be concluded that the thermal performance instability of piezoresistive pressure sensors is mainly attributable to the effects of temperature on the piezoresistive coefficient and resistances. It is observed that the simulated design of CNT pressure sensor induced an excellent model to compensate for temperature as well as the sensitivity is also increased.The pressure sensor is established to have an enhanced pressure output of 29% as compared to silicon pressure sensor at high temperature. The temperature compatibility of the sensor totally depends upon the sensing element. In this study , we have also presented two temperature compensation for high-temperature piezoresistive pressure sensors. Resistive compensation techniques includes additional silicon resistors and resistance of these resistors drops due to their negative TCR. Then the share of piezoresistors from supply voltage increases and drop in the undesired output voltage, coming from negative temperature coefficient of piezoresistive coefficient (TCP), is compensated. double bridge temperature compensation technique is suggested for tracking errors. Through simulation analysis the response of compensated and non-compensated sensors were investigated and concluded the the output voltage of the compensated pressure sensor is consistent against the variation of temperature.

Declarations

1. Funding: no funding is available for this publication.
2. Conflict of Interest: The authors declare that they have no conflict of interest.
3. Author contributions SS Gill given the concepts and helped in Implementations of work , Proof Rekha has done simulations and implemented the concept and written work
4. Compliance with ethical standards Paper is plagiarism free
- 5 Consent to participate : All authors given consents for the publication of this material
6. Consent for Publication : All authors given consents for the publication of this material
7. Acknowledgments : NA
8. Availability of data and material: Data and other supplement data will be available

References

1. Lou, L., Zhang, S., Park, W. T., Tsai, J. M., Kwong, D. L., & Lee, C. (2012). Optimization of NEMS pressure sensors with a multilayered diaphragm using silicon nanowires as piezoresistive sensing elements. *Journal of Micromechanics and Microengineering*, 22(5), 055012.
2. Sathyanarayanan, S., & Vimala Juliet, A. (2011). Simulation of Low-Pressure MEMS Sensor for Biomedical Application. *Journal of Nanotechnology in Engineering and Medicine*, 2(3).
3. Meena, K. V., Mathew, R., & Sankar, A. R. (2017). Design and optimization of a three-terminal piezoresistive pressure sensor for catheter-based in vivo biomedical applications. *Biomedical Physics & Engineering Express*, 3(4), 045003.
4. Xu, Y., Hu, X., Kundu, S., Nag, A., Afsarimanesh, N., Sapra, S., ... & Han, T. (2019). Silicon-based sensors for biomedical applications: a review. *Sensors*, 19(13), 2908.
5. Guan, T., Yang, F., Wang, W., Huang, X., Jiang, B., & Zhang, D. (2016). The design and analysis of piezoresistive Shuriken-structured diaphragm micro-pressure sensors. *Journal of Microelectromechanical systems*, 26(1), 206-214.5
6. Li, C., Cordovilla, F., Jagdheesh, R., & Ocaña, J. L. (2018). Design optimization and fabrication of a novel structural SOI piezoresistive pressure sensor with high accuracy. *Sensors*, 18(2), 439.
7. Zhao, X., Yu, Y., Li, D., & Wen, D. (2015). Design, fabrication, and characterization of a high-sensitivity pressure sensor based on nano-polysilicon thin-film transistors. *AIP Advances*, 5(12), 127216.
8. Ali, A., Khan, A., Ali, A., & Ahmad, M. (2017). Pressure-sensitive properties of carbon nanotubes/bismuth sulfide composite materials. *Nanomaterials and Nanotechnology*, 7, 18

9. Li, J., Zhang, C., Zhang, X., He, H., Liu, W., & Chen, C. (2020). Temperature Compensation of Piezo-Resistive Pressure Sensor Utilizing Ensemble AMPSO-SVR Based on Improved Adaboost. *RT. IEEE Access*, 8, 12413-12425.
10. Devi, R., Gill, S.S. A squared bossed diaphragm piezoresistive pressure sensor based on CNTs for low pressure range with enhanced sensitivity. *Microsyst Technol* (2021).
11. Katageri, A. C., & Sheeparamatti, B. G. (2015). Carbon Nanotube based Piezoresistive Pressure Sensor for Wide Range Pressure Sensing Applications-A Review. *International Journal of Engineering Research and*, 4(08), 27.
12. Helbling, T., Roman, C., Durrer, L., Stampfer, C., & Hierold, C. (2011). Gauge factor tuning, long-term stability, and miniaturization of nanoelectromechanical carbon-nanotube sensors. *IEEE transactions on electron devices*, 58(11), 4053-4060.
13. Tran, A. V., Zhang, X., & Zhu, B. (2019). Effects of temperature and residual stresses on the output characteristics of a piezoresistive pressure sensor. *IEEE Access*, 7, 27668-27676.
14. Balavalad, K. B., & Sheeparamatti, B. G. (2018, December). Design, Simulation & Analysis of Si, SOI & Carbon Nanotube (CNT) based Micro Piezoresistive Pressure Sensor for a High Temperature & Pressure. In *2018 International Conference on Circuits and Systems in Digital Enterprise Technology (ICCSDET)* (pp. 1-6). IEEE.
15. Sosa, J., Montiel-Nelson, J. A., Pulido, R., & Garcia-Montesdeoca, J. C. (2015). Design and optimization of a low power pressure sensor for wireless biomedical applications. *Journal of Sensors*, 2015.
16. Tran, A. V., Zhang, X., & Zhu, B. (2018). Mechanical structural design of a piezoresistive pressure sensor for low-pressure measurement: a computational analysis by increases in the sensor sensitivity. *Sensors*, 18(7), 2023.
17. Fung, C. K., Zhang, M. Q., Dong, Z., & Li, W. J. (2005, July). Fabrication of CNT-based MEMS piezoresistive pressure sensors using DEP nano assembly. In *5th IEEE Conference on Nanotechnology, 2005.* (pp. 199-202). IEEE.
18. Hierold, C., Jungen, A., Stampfer, C., & Helbling, T. (2007). Nano electromechanical sensors based on carbon nanotubes. *Sensors and Actuators A: Physical*, 136(1), 51-61.
19. Helbling, T., Roman, C., Durrer, L., Stampfer, C., & Hierold, C. (2011). Gauge factor tuning, long-term stability, and miniaturization of nanoelectromechanical carbon-nanotube sensors. *IEEE transactions on electron devices*, 58(11), 4053-4060.
20. Jang, D., Hong, Y., Hong, S., & Lee, J. H. (2019). A Novel Barometric Pressure Sensor Based on Piezoresistive Effect of Polycrystalline Silicon. *JOURNAL OF SEMICONDUCTOR TECHNOLOGY AND SCIENCE*, 19(2), 172-177.
21. Monea, B. F., Ionete, E. I., Spiridon, S. I., Ion-Ebrasu, D., & Petre, E. (2019). Carbon nanotubes and carbon nanotube structures used for temperature measurement. *Sensors*, 19(11), 2464.

22. Kerrou, F., Boukabache, A., & Pons, P. (2012). Modelling of thermal behavior N-doped silicon resistor..
23. Chiou, J. A., & Chen, S. (2007). Thermal hysteresis and voltage shift analysis for differential pressure sensors. *Sensors and Actuators A: Physical*, 135(1), 107-112.
24. Zhang, S., Wang, T., Lou, L., Tsang, W. M., Sawada, R., Kwong, D. L., & Lee, C. (2014). Annularly grooved diaphragm pressure sensor with embedded silicon nanowires for low pressure application. *Journal of Microelectromechanical Systems*, 23(6), 1396-1407.
25. Furlan, H., Fraga, M. A., Koberstein, L. L., & Rasia, L. A. Modeling of MEMS Piezoresistive Sensors. *Pesquisas Aplicadas em Modelagem Matemática*, 215-240.
26. Suja, K. J., Kumar, G. S., Nisanth, A., & Komaragiri, R. (2015). Dimension and doping concentration based noise and performance optimization of a piezoresistive MEMS pressure sensor. *Microsystem Technologies*, 21(4), 831-839.
27. Abdelaziz, B., Fouad, K., & Kemouche, S. (2014). The effect of temperature and doping level on the characteristics of piezoresistive pressure sensor. *Journal of Sensor Technology*, 4(2), 59.
28. Yao, Z., Liang, T., Jia, P., Hong, Y., Qi, L., Lei, C., & Xiong, J. (2016). A high-temperature piezoresistive pressure sensor with an integrated signal-conditioning circuit. *Sensors*, 16(6), 913.
29. Yao, Z., Liang, T., Jia, P., Hong, Y., Qi, L., Lei, C., ... & Xiong, J. (2016). Passive resistor temperature compensation for a high-temperature piezoresistive pressure sensor. *Sensors*, 16(7), 1142.
30. Liu, Y., Wang, H., Zhao, W., Qin, H., & Fang, X. (2016). Thermal-performance instability in piezoresistive sensors: Inducement and improvement. *Sensors*, 16(12), 1984.
31. Kayed, M. O., Balbola, A. A., & Moussa, W. A. (2019). A new temperature transducer for local temperature compensation for piezoresistive 3-D stress sensors. *IEEE/ASME Transactions on Mechatronics*, 24(2), 832-840.
32. Zhou, G., Zhao, Y., Guo, F., & Xu, W. (2014). A smart high accuracy silicon piezoresistive pressure sensor temperature compensation system. *Sensors*, 14(7), 12174-12190.

Figures

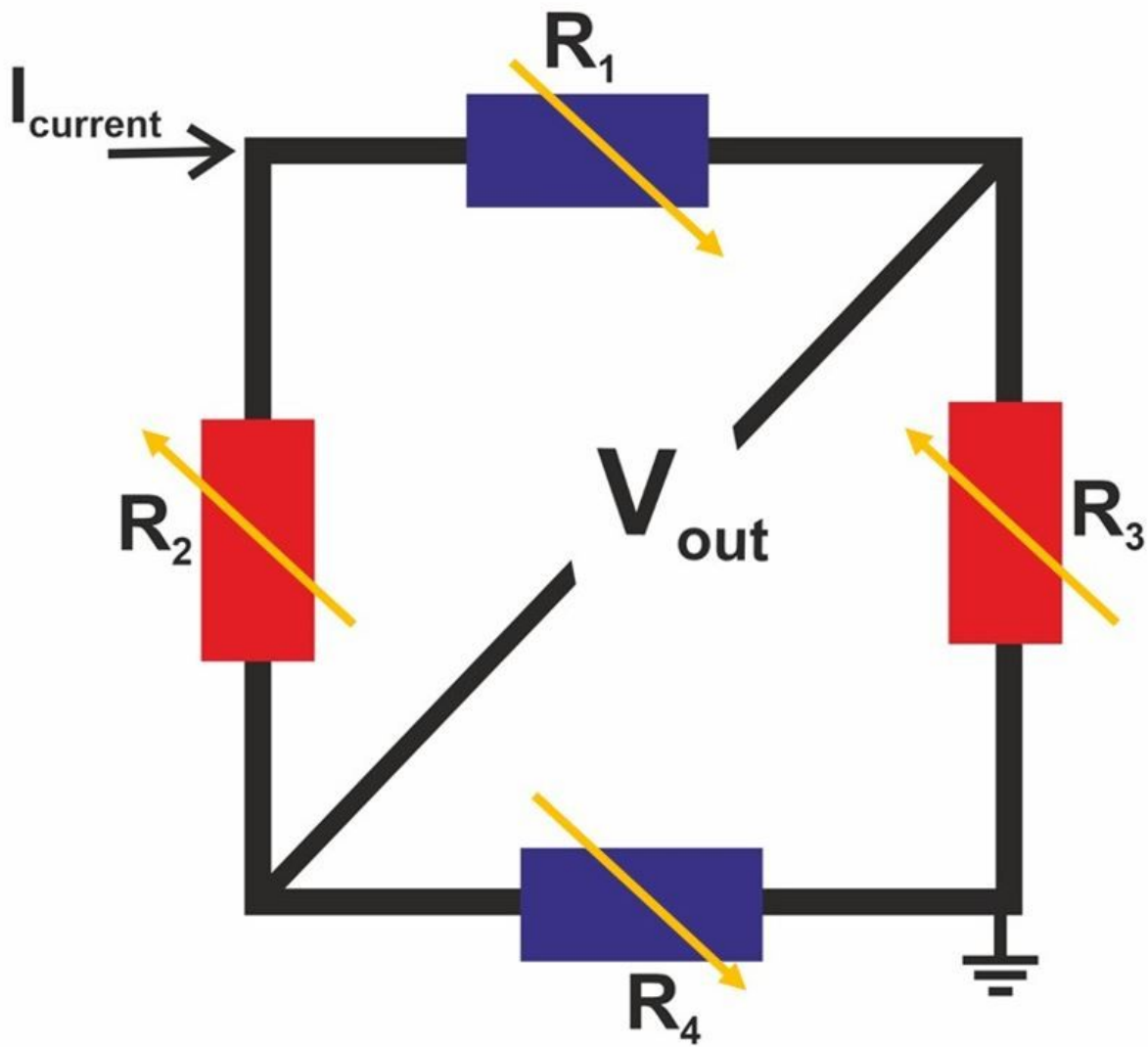


Figure 1

Equivalent Circuit of the piezoresistive pressure sensor

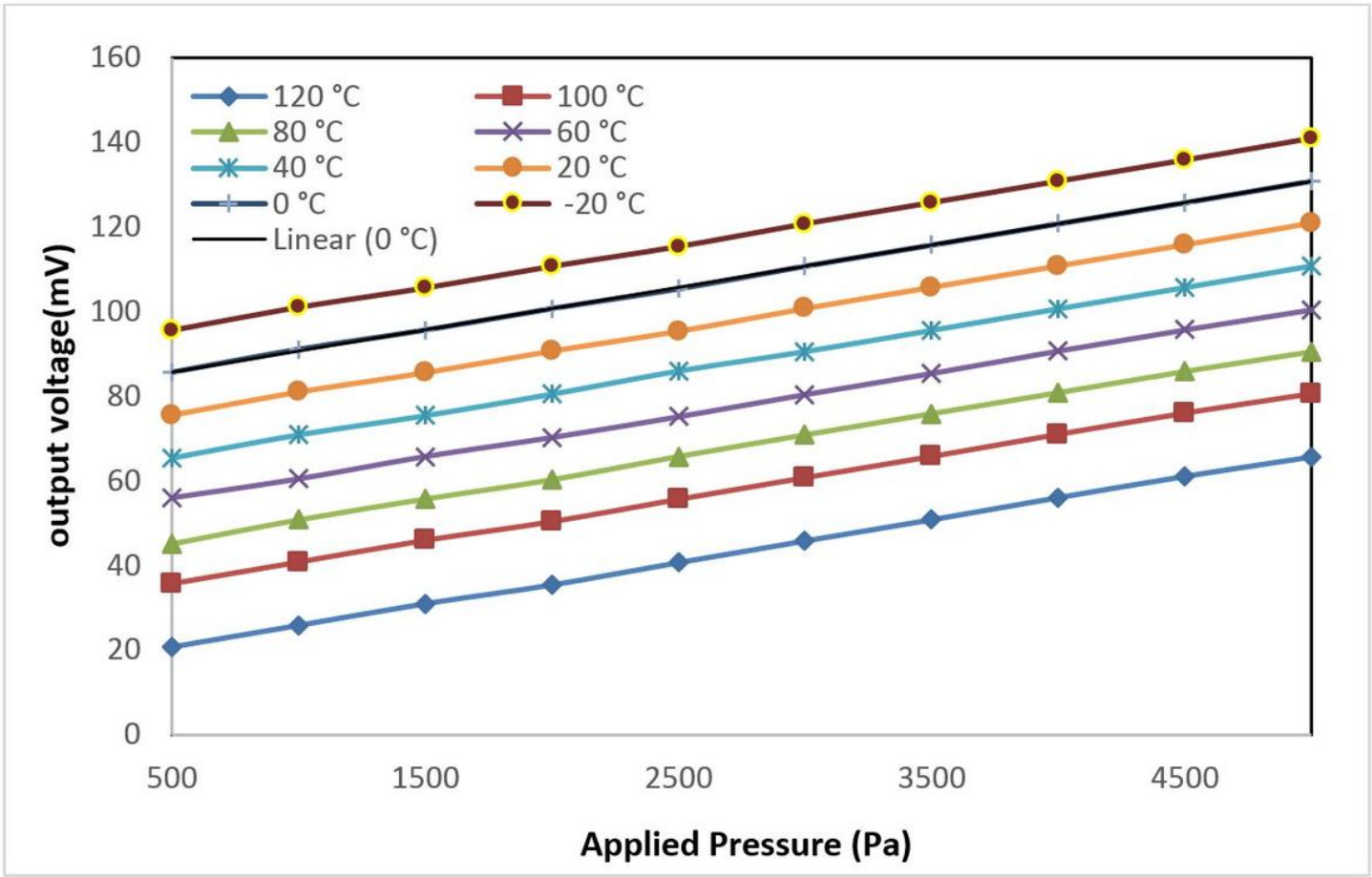


Figure 2

The Relationship between the output voltage and the applied pressure under various temperatures.

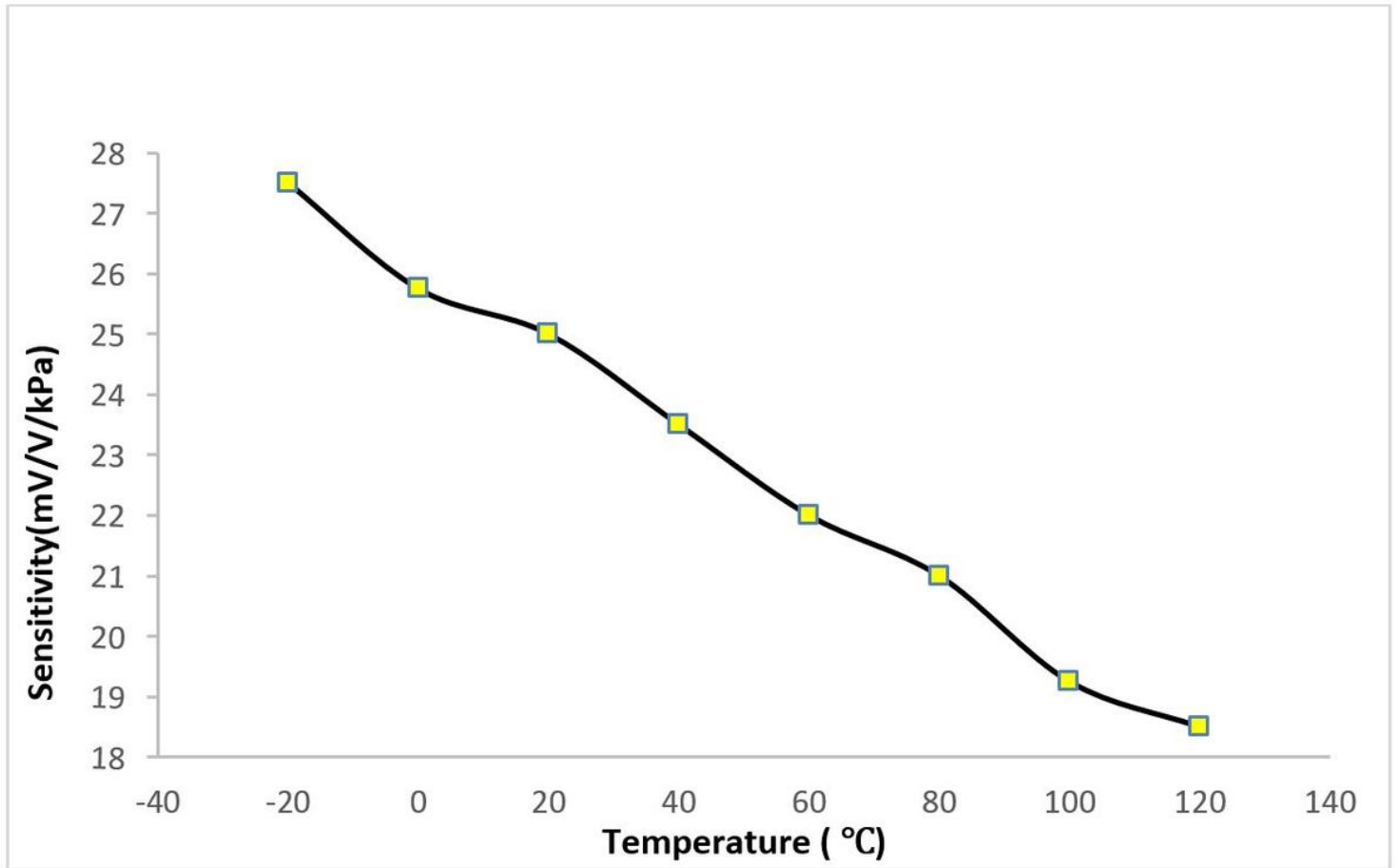


Figure 3

The relationship plot between the sensitivity of the pressure sensor and temperature variations.

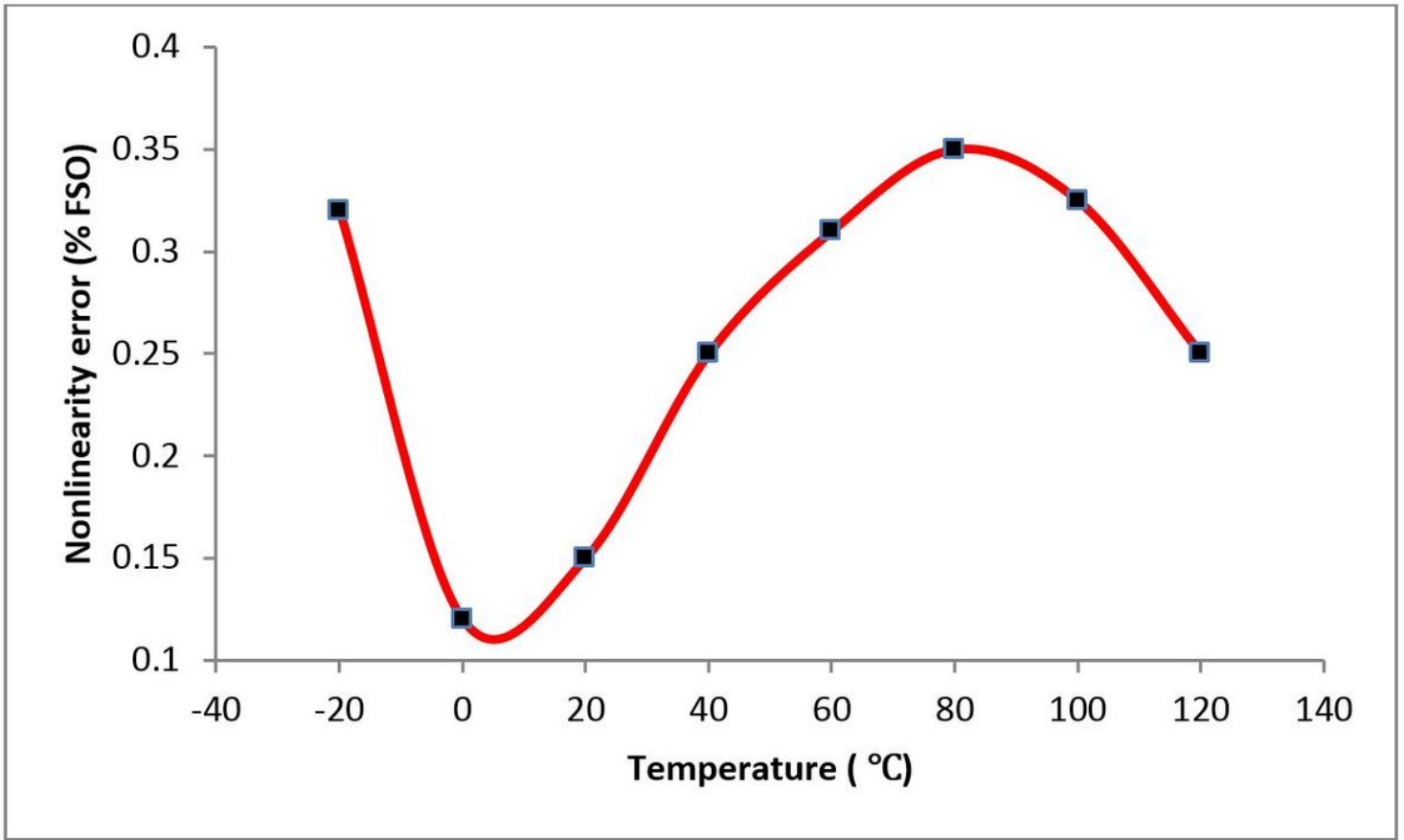


Figure 4

Nonlinearity error measurement of the pressure sensor and temperature variations.

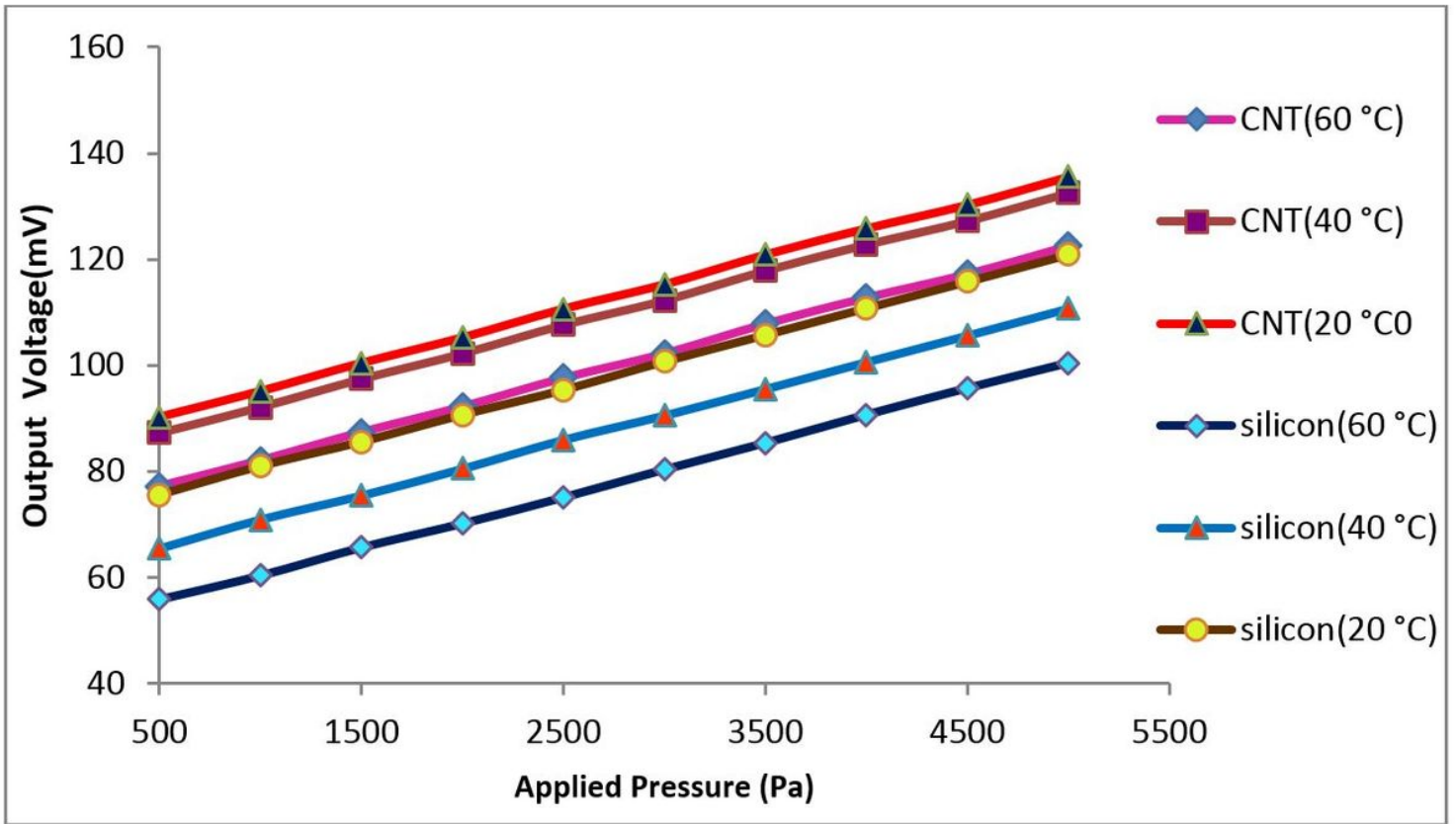


Figure 5

Comparative analysis of silicon and CNT as piezoresistive sensing elements at different temperature range.

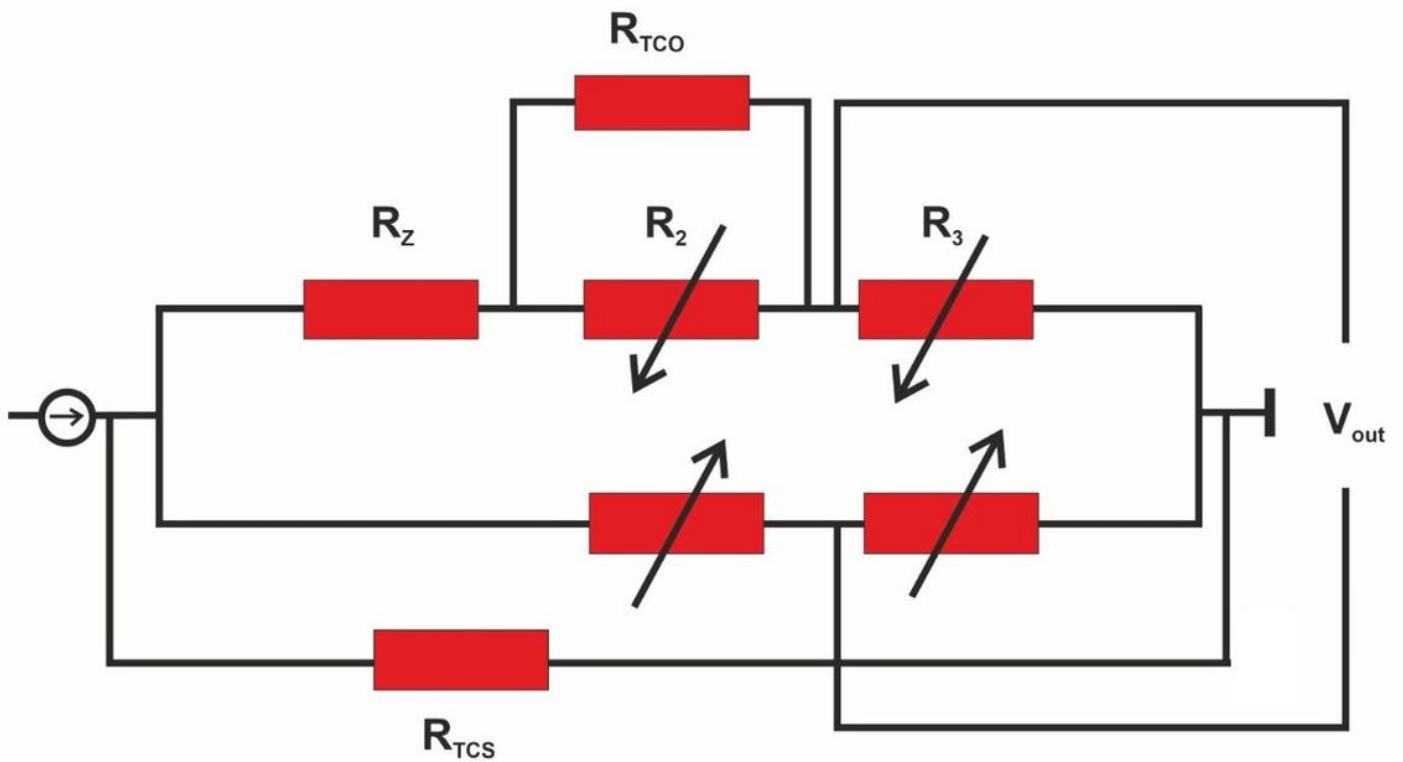


Figure 6

Schematic diagram of the resistive compensation network.

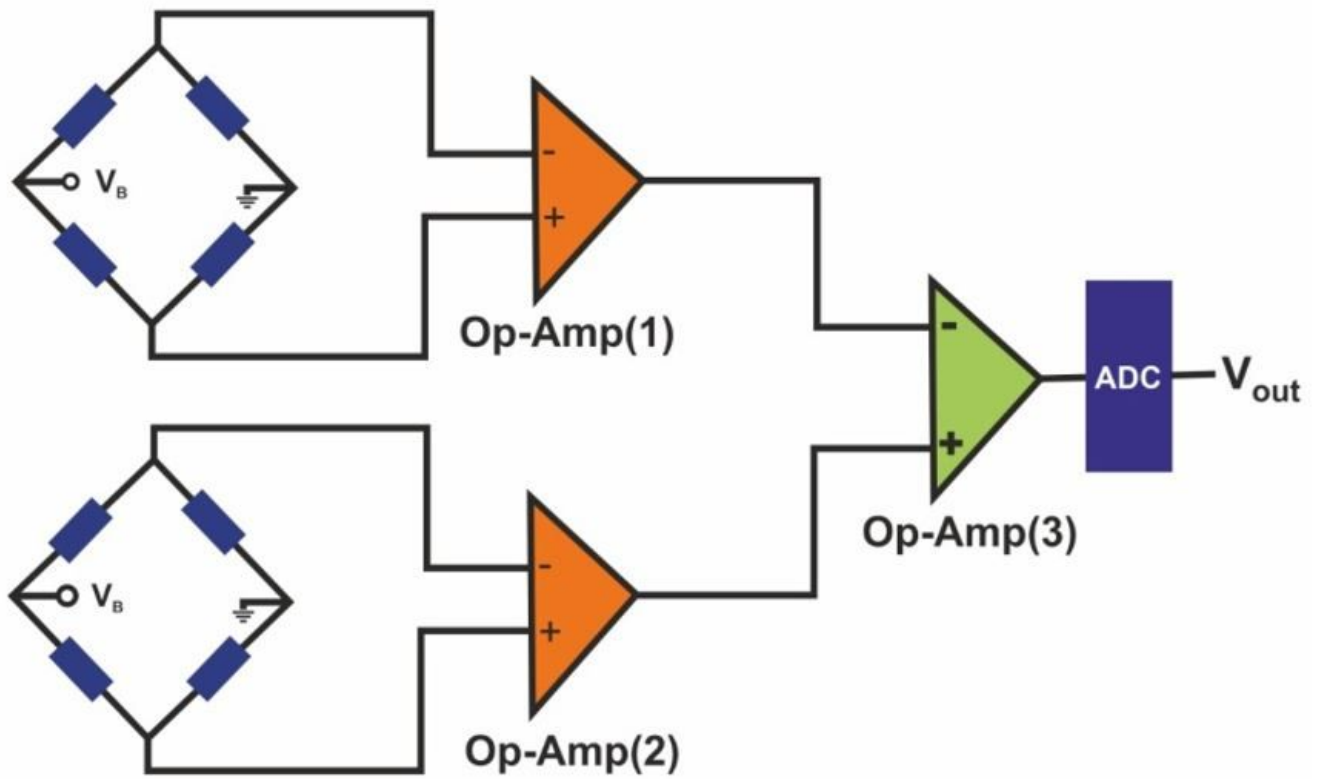


Figure 7

Schematic diagram of the Double bridge compensation network.

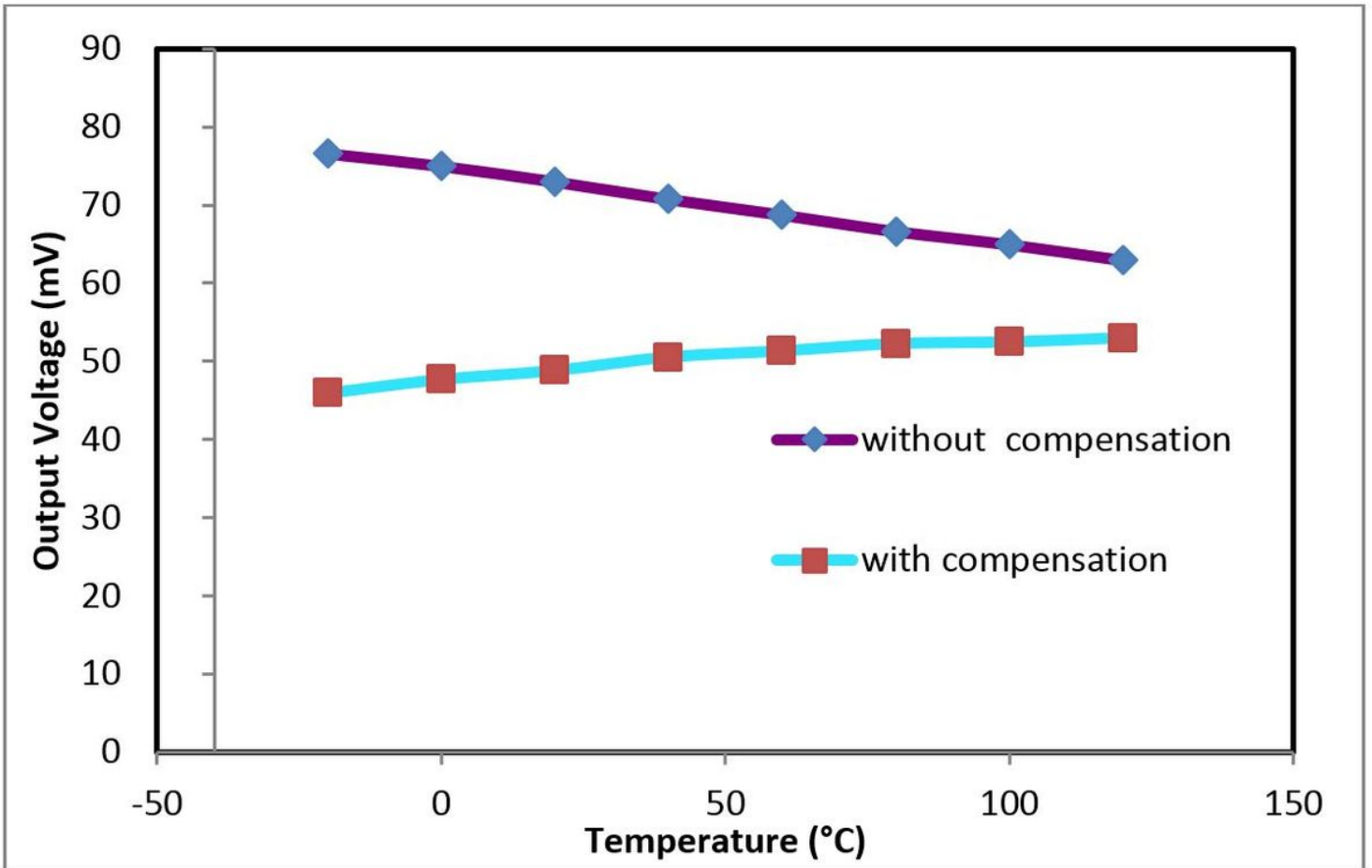


Figure 8

Output voltage with compensated and without compensated pressure sensor vs. temperature.